Chemical Engineering Journal 146 (2009) 148–154

Contents lists available at ScienceDirect

Chemical Engineering Journal

journal homepage: www.elsevier.com/locate/cej

Kinetics of high-temperature water-gas shift reaction over two iron-based commercial catalysts using simulated coal-derived syngases

San Shwe Hla[a,*], D. Park[a], G.J. Duffy[b], J.H. Edwards[b], D.G. Roberts[a], A. Ilyushechkin[a], L.D. Morpeth[a], T. Nguyen[a]

[a] CSIRO Energy Technology, PO Box 883, Pullenvale, QLD 4069, Australia
[b] CSIRO Energy Technology, PO Box 330, Newcastle 2300, Australia

ARTICLE INFO

Article history:
Received 6 August 2007
Received in revised form 5 September 2008
Accepted 17 September 2008

Keywords:
Kinetics
Water-gas shift reaction
Fe–Cr oxide catalyst
Coal-derived syngas

ABSTRACT

The kinetics of the water-gas shift (WGS) reaction over two iron–chromium based commercial catalysts has been studied. The experiments were performed in a differential reactor at a constant temperature of 450 °C and a space velocity of 1.9 $m^3\ g_{cat}^{-1}\ h^{-1}$ at approximately atmospheric pressure. The effects of CO, CO_2, H_2O and H_2 concentration on WGS reaction rate were determined over both catalysts using selected gas compositions that might be encountered in coal based gasification system of the dry-feed and slurry-feed types and at the backend of conventional fixed-bed and catalytic membrane reactors.

It was found that the rates of the WGS reaction (in mol $g_{cat}^{-1}\ s^{-1}$) over two commercial catalysts (referred to as HTC1 and HTC2) at a reaction temperature of 450 °C can be expressed by the following power-law rate models:

For HTC1

$$R = 10^{2.845\pm0.03} \exp\left(\frac{-111\pm2.63}{R'T}\right) P_{CO}^{1.0\pm0.031} P_{CO_2}^{-0.36\pm0.043} P_{H_2}^{-0.09\pm0.007} \left(1-\frac{1}{K}\frac{P_{CO_2}P_{H_2}}{P_{CO}P_{H_2O}}\right)$$

For HTC2

$$R = 10^{0.659\pm0.0125} \exp\left(\frac{-88\pm2.18}{R'T}\right) P_{CO}^{0.9\pm0.041} P_{H_2O}^{0.31\pm0.056} P_{CO_2}^{-0.156\pm0.078} P_{H_2}^{-0.05\pm0.006} \left(1-\frac{1}{K}\frac{P_{CO_2}P_{H_2}}{P_{CO}P_{H_2O}}\right).$$

It was observed that HTC1 promotes the rate of WGS reaction when the inlet gas consists of higher CO concentration, and lower CO_2 and H_2 concentration. Due to the less-negative reaction order with respect to CO_2, HTC2 was found to be more applicable to the gas streams with higher CO_2 levels, which are likely to be found on the retentate side at the backend of a catalytic membrane reactor.

1. Introduction

An important step in the processing of coal-derived syngases, both as a precursor to fuel gas decarbonisation and for adjusting the CO/H_2 ratio for downstream synfuel production, is the water-gas shift (WGS) reaction involving the reaction of CO with steam to produce CO_2 and H_2:

$$CO(g) + H_2O(g) \leftrightarrow CO_2(g) + H_2(g) \quad \Delta H_{298\,K} = -41.1\ kJ\ mol^{-1} \quad (1)$$

The iron-based catalyst typically used for the high-temperature (HT) WGS reaction has changed little since the days when BASF first developed them in the early twentieth century [1] and works extremely well in industrial application for natural gas-derived syngases where the CO concentrations are in the range 5–10%.

However, in the case of coal-derived syngases where the CO concentration is relatively high (~40–60%), a considerably higher degree of shifting is required. This work, as part of a wider program studying catalysts for use in near-zero emission energy systems, seeks to measure the performance of commercially available catalysts under conditions relevant to coal-derived syngases. In particular, it seeks to characterise the performance of two high-temperature catalysts from two different commercial suppliers in atmospheres that have high concentrations of H_2 or CO_2 (such as those which might be encountered in a packed-bed membrane reactor application).

Studying the kinetics of the WGS reaction under specific and well-controlled operating conditions provides important information not only for the understanding of the mechanism of catalysis

* Corresponding author. Tel.: +61 7 3327 4125; fax: +61 7 3327 4455.
E-mail address: san.hla@csiro.au (S.S. Hla).

1385-8947/$ – see front matter.
doi:10.1016/j.cej.2008.09.023

itself, but also for the design and optimisation of the reactor system. A number of different kinetic rate expressions have been reported and tested to evaluate the WGS reaction rate [2–10]. According to Fott et al. [2], over 20 different kinetic equations have been proposed and there is still a lack of consensus over the nature and role of active sites and the reaction mechanism.

There are some excellent reviews of WGS reaction kinetics [11,12] in the literature. Podolski and Kim [12] re-examined six WGS reaction expressions and associated published data and concluded that only the Langmuir–Hinshelwood and the power-law models could accurately describe the reaction behaviour over the temperature and concentration ranges investigated. Compared to the Langmuir–Hinshelwood (LH) based WGS reaction rate expression (which is derived from detailed and specific reaction mechanisms), the power-law rate expression is often used as a relatively simple approximation of the rate equation, usually valid for a specific range of conditions. Podolski and Kim [12] also suggested that a power-law model is a reasonable alternative to the LH model. Several studies [1,5,13,14] have demonstrated the usefulness of a simple empirical power-law expression as a tool for an integrated and optimised simulation of a fuel processing system and for reactor design studies. A power-law form has therefore been used to model the WGS kinetics measured in this study.

The power-law expression is generally of the form:

$$R = kP_{CO}^{a}P_{H_2O}^{b}P_{CO_2}^{c}P_{H_2}^{d}(1-\beta) \quad (2)$$

where, R = reaction rate (mol g_{cat}^{-1} s^{-1}); a, b, c, d = reaction order of CO, H_2O, CO_2, H_2 respectively; k = rate constant = $A\exp(-E/R'T)$; R' = universal gas constant (kJ mol^{-1} K^{-1}); A = pre-exponential factor; E = activation energy (kJ mol^{-1}); T = reaction temperature (K)

β is defined as

$$\beta = \frac{1}{K}\frac{P_{CO_2}P_{H_2}}{P_{CO}P_{H_2O}} \quad (3)$$

where K is the equilibrium constant for the WGS reaction.

The aims of the present work are two-fold. The first is to examine the relative performance of two high-temperature commercial catalysts under selected syngas compositions that are consistent with those that might be encountered when a WGS reactor is operated downstream of a coal gasifier. The second is to obtain accurate kinetic parameters through which the catalytic capability of these catalysts can be assessed in reactor modelling studies.

The study is directed at assessing the performance of these catalysts in:

(a) a conventional fixed-bed WGS reactor where any gas separation would take place downstream of the reactor;
(b) in a membrane reactor which is packed with catalyst and which allows hydrogen to be removed as it is produced, thus driving the equilibrium to the right.

The latter option has significant implications for the gas compositions that the catalyst will experience at the backend of the reactor.

2. Experimental

2.1. Water-gas shift reactor system

A schematic diagram of the experimental apparatus and the configuration of the fixed-bed reactor are shown in Fig. 1. The reactor was capable of operation at temperatures up to 1200 °C and pressures up to 1.6 MPa. The reaction tube (13.0 mm ID and 1000 mm length) was made from quartz, and housed within a stainless steel pressure tubing. A weighed sample of catalyst was packed in the reactor between layers of inert material (quartz wool). The mass flow rate was controlled and measured using mass flow controllers. A HPLC (High Performance Liquid Chromatography) pump (Shimadzu LC-20AT) was used to generate a steady flow of water for steam production. The gas was electrically heated and maintained at about 160 °C prior to entry to the furnace. De-ionised water was used for the HPLC pump, and was continuously filtered before being introduced to the pump. Concentrations of product gases (CO, CO_2, H_2 and N_2) were determined by gas chromatography (Varian CP-4900).

2.2. Catalyst sample

Both High-Temperature Catalyst 1 (HTC1) and High-Temperature Catalyst 2 (HTC2) are copper promoted iron–

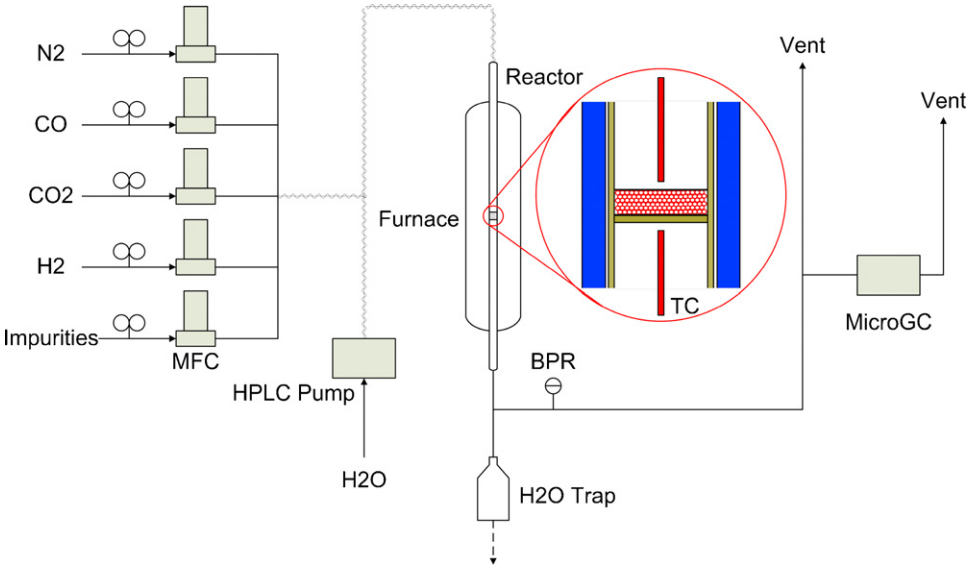

Fig. 1. Schematic diagram of the reaction system and fixed-bed reactor used for WGS catalytic reactions.

Table 1
Specifications of HTC1 and HTC2.

Catalyst	HTC1	HTC2
Composition		
Fe_2O_3	80–90%	80–95%
Cr_2O_3	8–13%	5–10%
CuO	1–2%	1–5%
Shape [commercially available]	Pellet	Pellet
Size (diameter × height) [commercially available]	6 mm × 6 mm	6 mm × 6 mm

chromium oxide based high-temperature shift catalysts purchased from commercial suppliers. Vendor-supplied details for these catalysts are given in Table 1. Both catalysts have high iron content, and have slight difference in copper and chromium concentration in the oxides. The catalyst pellets were ground and sieved to a particle size of +53–150 μm to reduce the possibility of internal diffusion limitations on the rate measurements.

2.3. Selection of syngas compositions and operating temperature

The syngas compositions to be investigated in this study have been chosen to be consistent with those that might be encountered in both a dry-feed Shell-type gasifier and a slurry-feed Texaco-type gasifier. Fifteen data sets of syngas compositions (8 for Shell-type and 7 for Texaco-type gasifiers) were obtained from literature, including those for Australian black coals in Shell (3 data sets) and Texaco (1 data set) gasifiers [15,16]. Table 2 describes the average syngas compositions from Shell-type gasifiers (dry-feed) and Texaco-type gasifiers (slurry-feed). Gas composition of the outlet of conventional fixed-bed WGS reactor (post-WGS reaction) was determined on the basis of the stoichiometry of the reactions assuming CO conversion level is 90%, while the gas composition of the backend of a catalytic membrane reactor (post-hydrogen separation) was calculated assuming 90% CO conversion and 90% H_2 removal.

In this study, steam was added to all gas mixtures listed in Table 2 to give a constant inlet steam:carbon molar ratio of 3:1.

The vendor's manual on HTC1 mentions that loss in activity of the catalyst is possible at a temperature greater than 470 °C. Based on this information, an operating temperature of 450 °C was used for all the experimental runs in this study.

2.4. Test procedure

Approximately 0.2 g of catalyst was mixed with approximately 1 g of alpha-alumina of the same particle size and the mixture was placed on the sample bed. To check the catalytic activity of alpha-alumina, an experiment was carried out by loading 1 g of alpha-alumina only and, no significant CO conversion was observed within the range of test conditions selected in this study. Initial reduction was carried out using a gas mixture containing 9.0% H_2, 4.5% CO, 45% N_2 and 41.5% H_2O with a gas velocity of 5.1 cm s^{-1} at 250 °C for 2 h. For the catalyst performance tests and kinetic measurement tests, the sample was heated to the desired temperature under nitrogen and steam, and a gas mixture with specified composition was introduced to the reactor. The reactor was operated with this test atmosphere for 5–6 h or until measurements became stable.

Table 2
Experimental inlet gas composition (dry basis) used in this study.

Conditions	CO (%)	H_2 (%)	CO_2 (%)	N_2 (%)
Dry-feed coal-derived syngas	65	30	2	3
Slurry-feed coal-derived syngas	44	37	16	3
Backend of catalytic membrane reactor (retentate side)	7	12	78	3
Backend of WGS reactor	4	55	38	3

3. Results and discussion

3.1. Initial test to define differential reactor conditions

To determine what operating conditions are required to achieve a differential mode of operation, tests were conducted over a range of gas flows and sample loading which control the residence time and level of CO conversion. Lei [17] has recommended that CO conversion should be less than 10% to ensure operation in a differential mode. After a series of initial tests were carried out using HTC1 with the dry-feed coal-derived syngas composition, CO conversion below 10% was achieved with the use of a total inlet dry gas flow rate to the reactor of approximately 800 mL (STP)/min and 0.2 g of catalyst (calculated wet gas velocity and space velocity at 450 °C are 79.7 cm s^{-1} and 1.9 m^3 $g_{cat}{}^{-1}$ h^{-1} respectively). Based on this finding, operating conditions for the HTC1 and HTC2 performance tests on four selected gas inlet compositions were defined as shown in Table 3 by keeping constant wet gas velocities and constant H_2O:carbon molar ratio.

3.2. Performance of HTC1 and HTC2 on four selected gas inlet compositions

Fig. 2 shows the performance of HTC1 and HTC2 at the four inlet gas compositions with a constant wet gas velocity. It should be noted that data presented in Fig. 2 represent the last 30 data points (interval between each data point was approximately 3 min) of each experimental run when the reactor was running under steady state conditions. Upper and lower confidence limits were calculated at a 95% confidence level. From Fig. 2, similar performance of HTC1 and HTC2 on four selected gas inlet compositions can be observed. Results show that the highest CO conversion was achieved under dry-feed coal-derived syngas composition where inlet gas CO content was highest, and the lowest CO conversion was found with the backend of WGS reactor gas composition where inlet gas CO content was lowest. HTC1 was found to give better performance than HTC2 on dry-feed coal-derived syngas and slurry-feed coal-derived syngas, while HTC2 performance under 'backend of the retentate side of catalytic membrane reactor' conditions was bet-

Table 3
Experimental conditions for four different inlet gas compositions tested under constant space velocity of 1.9 m^3 $g_{cat}{}^{-1}$ h^{-1} at 450 °C.

Conditions	Flow rate (mL/min) at STP					Water pumping rate (mL/min)
	CO	H_2	CO_2	N_2	Total dry-gas	
Dry-feed coal-derived syngas	518	239	16	24	797	1.288
Slurry-feed coal-derived syngas	377	317	137	26	857	1.240
Backend of catalytic membrane reactor (retentate side)	47	81	526	20	674	1.382
Backend of WGS reactor	42	584	404	32	1062	1.076
Catalyst weight = 0.2 g, Inert diluting material (alpha-alumina) = 1.0 g						

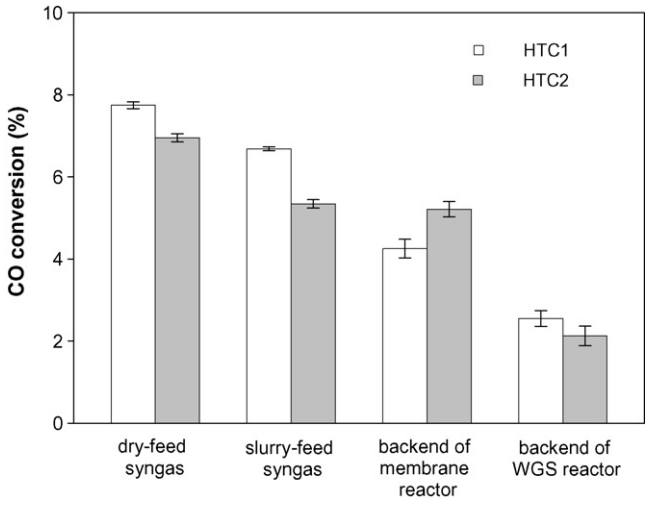

Fig. 2. CO conversion profile during WGS reaction for four different inlet gas compositions (reacting temperature = 450 °C, 0.2 g of catalyst, wet gas velocity = 79.7 cm s^{-1} and steam:carbon ratio of 3).

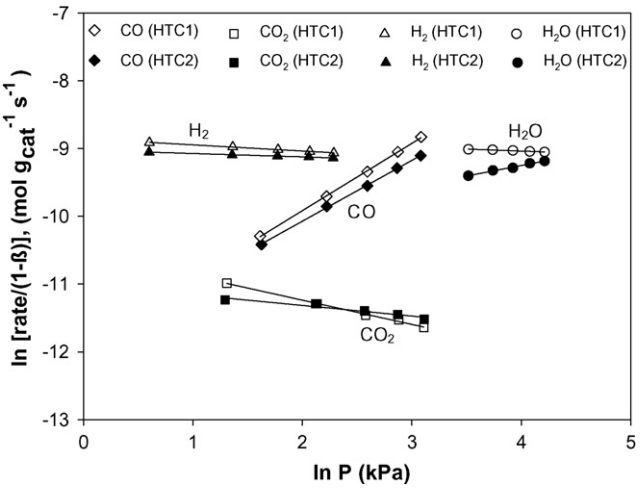

Fig. 3. Log–log plots for the effect of CO, CO_2, H_2 and H_2O partial pressures on reaction rates over HTC1 and HTC2 using selected gas compositions (Tables 4 and 5) at 450 °C.

ter than that of HTC1. It is interesting to note that dry-feed and slurry-feed coal-derived syngases contain low CO_2 content and the selected gas composition for the backend of catalytic membrane reactor contains high CO_2 concentration. Detailed results regarding effects of individual gas species on WGS reaction kinetics over HTC1 and HTC2 are discussed in the next section.

3.3. Kinetics of the water-gas shift reaction over HTC1 and HTC2 at 450 °C

An empirical power-law expression (Eq. (2)) is often used to describe the kinetics of WGS catalysts. In the current study on HTC1 and HTC2, the kinetics is expected to be affected by the presence of both reactants and products. The rate data measured for WGS reaction at 450 °C (723 K) are based on dry-feed coal-derived syngas and backend of the WGS reactor conditions and those measurements are summarised in Tables 4 and 5. Note that in each set of data the composition of only one component varies (shown in bold) while all other compositions are held constant. β in Tables 4 and 5 is the term reflecting the reverse reaction or approach to equilibrium, calculated using Eq. (3). The equilibrium constant for the WGS reaction for a wide range of reaction temperatures is given by Twigg [4] and the calculated equilibrium constant of the WGS is 7.3369 at 450 °C.

Fig. 3 presents plots of ln [WGS reaction rate/$(1-\beta)$] versus ln of component partial pressure over HTC1 and HTC2. It can be seen that all the plots are linear, confirming that the empirical power rate law equation is suitable for modelling the kinetics of the WGS reaction over HTC1 and HTC2. The slope of each straight line of the log–log plots can be used to determine the reaction order with respect to individual species. From Fig. 3, the reaction orders with respect to CO, H_2O, CO_2 and H_2 over HTC1 and HTC2 were calculated; and these values are listed in Table 6. The reaction orders

Table 4
Kinetic data measured from WGS reaction over HTC1 with dry-feed coal-derived syngas and backend of catalytic membrane reactor conditions.

P_{CO} (kPa)	P_{H_2O} (kPa)	P_{CO_2} (kPa)	P_{H_2} (kPa)	P_{N_2} (kPa)	β	CO conversion rate (CO mol g^{-1} s^{-1})
CO order data [base case = dry-feed coal-derived syngas]						
21.85	67.50	0.90	9.90	1.17	0.0008	1.46E−04
17.66	67.31	0.88	9.86	5.62	0.001	1.17E−04
13.37	67.46	0.86	9.74	9.89	0.0013	8.78E−05
9.21	67.47	0.85	9.72	14.08	0.0018	6.09E−05
5.02	67.62	0.83	9.66	18.20	0.0032	3.38E−05
H_2O order data [base case = dry-feed coal-derived syngas]						
21.81	**67.57**	0.90	9.85	1.20	0.0008	1.17E−04
21.59	**59.01**	0.89	9.91	9.93	0.0009	1.18E−04
21.49	**50.59**	0.89	10.00	18.37	0.0011	1.20E−04
21.52	**42.06**	0.88	10.11	26.75	0.0013	1.21E−04
21.50	**33.69**	0.89	10.18	35.07	0.0017	1.22E−04
CO_2 order data [base case = backend of catalytic membrane reactor]						
2.06	72.38	**3.70**	3.53	19.67	0.012	1.68E−05
2.03	72.53	**8.45**	3.48	14.83	0.0272	1.21E−05
2.02	72.49	**13.16**	3.45	10.21	0.0422	1.01E−05
2.00	72.48	**17.81**	3.42	5.61	0.0574	9.31E−06
1.99	72.53	**22.39**	3.38	1.04	0.0714	8.17E−06
H_2 order data [base case = dry-feed coal-derived syngas]						
21.39	67.38	0.88	**1.83**	9.85	0.0002	1.35E−04
21.36	67.46	0.88	**3.91**	7.72	0.0003	1.27E−04
21.44	67.51	0.88	**5.91**	5.58	0.0005	1.22E−04
21.60	67.49	0.89	**7.90**	3.44	0.0007	1.18E−04
21.78	67.61	0.90	**9.84**	1.19	0.0008	1.16E−04

Table 5
Kinetic data measured from WGS reaction over HTC2 with dry-feed coal-derived syngas and backend of catalytic membrane reactor conditions.

P_{CO} (kPa)	P_{H_2O} (kPa)	P_{CO_2} (kPa)	P_{H_2} (kPa)	P_{N_2} (kPa)	β	CO conversion rate (CO mol g^{-1} s^{-1})
CO order data [base case = dry-feed coal-derived syngas]						
21.79	67.57	0.91	9.79	1.27	0.0008	1.11E−04
17.55	67.51	0.88	9.70	5.68	0.0010	9.22E−05
13.38	67.46	0.87	9.65	9.97	0.0013	7.11E−05
9.23	67.47	0.85	9.63	14.15	0.0018	5.26E−05
5.09	67.41	0.84	9.63	18.36	0.0032	2.99E−05
H_2O order data [base case = dry-feed coal-derived syngas]						
21.82	**67.55**	0.91	9.81	1.24	0.0008	1.02E−04
21.59	**59.03**	0.89	9.86	9.96	0.0009	9.91E−05
21.52	**50.55**	0.89	9.97	18.40	0.0011	9.26E−05
21.50	**42.13**	0.89	10.06	26.75	0.0013	8.93E−05
21.52	**33.65**	0.88	10.14	35.14	0.0017	8.24E−05
CO_2 order data [base case = backend of catalytic membrane reactor]						
2.09	72.51	**3.64**	3.50	19.58	0.0115	1.31E−05
2.07	72.57	**8.35**	3.47	14.86	0.0262	1.22E−05
2.06	72.54	**13.02**	3.43	10.27	0.0408	1.08E−05
2.05	72.53	**17.64**	3.41	5.70	0.0551	1.01E−05
2.05	72.58	**22.51**	3.40	0.79	0.0702	9.26E−06
H_2 order data [base case = dry-feed coal-derived syngas]						
21.39	67.34	0.89	**1.82**	9.89	0.0002	1.17E−04
21.38	67.40	0.89	**3.89**	7.76	0.0003	1.12E−04
21.45	67.47	0.89	**5.89**	5.63	0.0005	1.11E−04
21.57	67.52	0.90	**7.84**	3.50	0.0007	1.09E−04
21.80	67.57	0.91	**9.79**	1.26	0.0008	1.07E−04

Table 6
Summary of kinetic rate constants for the WGS reaction on HTC1 and HTC2.

Catalyst	Apparent reaction orders				A[a]	E (kJ mol^{-1})
	a [CO]	b [H_2O]	c [CO_2]	d [H_2]		
HTC1	1.0 ± 0.031	0.0	−0.36 ± 0.043	−0.09 ± 0.007	700 ± 50	111 ± 2.63
HTC2	0.9 ± 0.041	0.31 ± 0.056	−0.156 ± 0.078	−0.05 ± 0.006	4.557 ± 0.133	88 ± 2.18

±Values in Table 6 represents the 95% confidence interval of the values of slope of the plots presented in Figs. 3 and 4.
[a] Unit in mol g(catalyst)$^{-1}$ s^{-1} $kPa^{-(a+b+c+d)}$.

obtained in this study generally agree well with those given in literature in which inlet CO concentrations are lower than dry-feed coal-derived syngas and slurry-feed coal-derived syngas used in this study. For both high-temperature catalysts, the rate of the WGS reaction is approximately proportional to the CO concentration (i.e., a is ∼1); the rate is retarded by increasing CO_2 concentration (c is negative) and, increasing H_2 concentration causes a slight reduction in reaction rate (d is slightly negative). From Table 6, it can be seen that reaction order with respect to CO_2 is significantly less negative in the case of HTC2 compared with that of HTC1. This reflects the higher conversions achieved with HTC2 when CO_2 concentration is high, i.e., at the composition corresponding to the backend of the membrane reactor.

Podolski and Kim [12] found the WGS reaction rate to be independent of steam concentration when it is in excess of the stoichiometric amount. This is true for the case of HTC1 in the current work, where we have found that the effect of changes in H_2O concentration is insignificant and its reaction order can be taken as zero for H_2O:carbon ratios greater than 1.5:1. However, it is interesting that the H_2O reaction order determined using HTC2 was found to be significantly positive even at high H_2O: carbon ratios. This difference could be associated with the microstructure of each catalyst and with the compositional difference between two high-temperature catalysts.

To obtain the apparent activation energy, an experiment was carried out where temperature was ramped from 360 to 450 °C with a heating rate of 0.5 °C/min. The results are presented in Fig. 4. The heating rate was slow enough that steady state conditions were approximated throughout the run. Logarithmic values of WGS reaction rates are plotted against inverse temperature values in Fig. 4. The values of slopes ($-E/R$) of the linear plots were determined through linear least-square-fitting techniques, and were found to be −13,336 and −10,605 for HTC1 and HTC2, which give an apparent activation energy of 111 and 88 kJ mol^{-1} respectively. As presented in Table 1, concentration of copper in HTC2 is higher than that in HTC1. The addition of copper decreases the activation energy of the catalyst and this finding is in agreement with experimen-

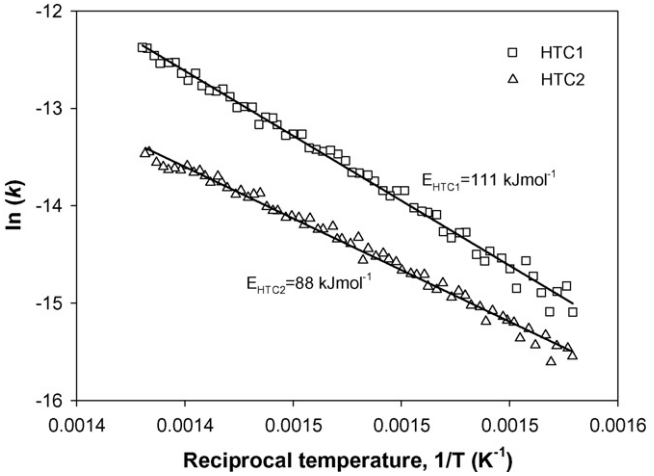

Fig. 4. Arrhenius plot for WGS reaction (dry-feed coal-derived syngas, 360–450 °C, 0.2 g each of HTC1 and HTC2, and steam:carbon ratio of 3).

tal results reported by Rhodes et al. [18]. The high values of the apparent activation energies (88 and 111 kJ mol^{-1}) suggest that both catalysts were operated under conditions largely free from the influence of mass transfer limitations through the pores of the particles. According to Keiski et al. [5], the values obtained with small catalyst particles are generally in the range of 100–113 kJ mol^{-1}, which is a good approximation to the results obtained in this work given the errors in such calculations. It is, however, very difficult to decrease particle size to a value where mass transfer effects can be completely eliminated [17].

The reaction rate orders obtained from slopes of plots in Fig. 3 can be used in conjunction with a rearrangement of Eq. (2) to obtain the rate constant (k) for the WGS reaction. The pre-exponential factor A at 450 °C can then be determined using k and the activation energy E. The power-law reaction rate expressions for WGS reaction over HTC1 and HTC2 at 450 °C under selected inlet conditions can be described as follows:

For HTC1

$$R = 10^{2.845\pm0.03} \exp\left(\frac{-111 \pm 2.63}{R'T}\right) P_{CO}^{1.0\pm0.031} P_{CO_2}^{-0.36\pm0.043} P_{H_2}^{-0.09\pm0.007} \left(1 - \frac{1}{K}\frac{P_{CO_2}P_{H_2}}{P_{CO}P_{H_2O}}\right)$$

For HTC2

$$R = 10^{0.659\pm0.0125} \exp\left(\frac{-88 \pm 2.18}{R'T}\right) P_{CO}^{0.9\pm0.041} P_{H_2O}^{0.31\pm0.056} P_{CO_2}^{-0.156\pm0.078} P_{H_2}^{-0.05\pm0.006} \left(1 - \frac{1}{K}\frac{P_{CO_2}P_{H_2}}{P_{CO}P_{H_2O}}\right)$$

for T = 450 °C (723 K)

where R' = 8.3144 × 10^{-3} kJ mol^{-1} K^{-1}.

Comparison between reaction rates calculated using the above expressions and those obtained from experimental results are shown in Fig. 5. The calculated rates fit the experimental values well, especially for HTC2 with an R^2 value of 0.996. The agreement between the experimental results for HTC1 and the calculated values is not as good as HTC2 (R^2 value of 0.973). This difference may relate to the variable performance of HTC1 which was found to vary slightly under identical experimental conditions on consecutive days.

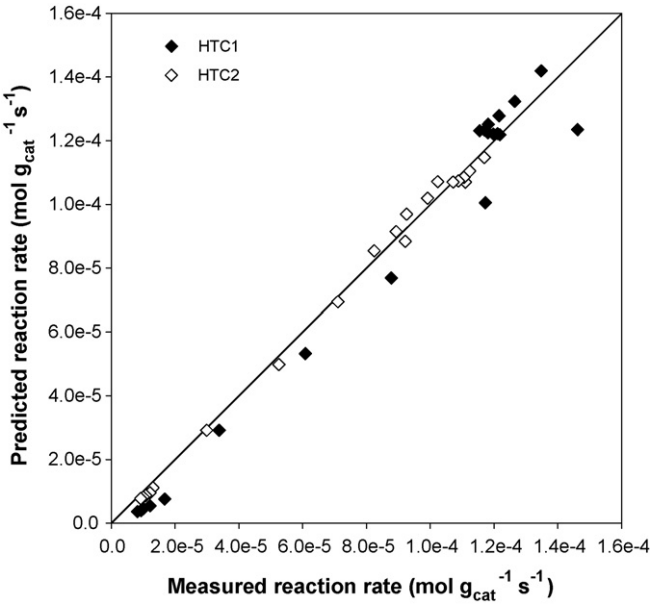

Fig. 5. Observed rate vs. predicted rates of water-gas shift over HTC1 and HTC2 under 450 °C and selected inlet compositions.

Table 7
Percentage reduction in reaction rate level due to WGS reverse reaction.

Rate w/o reverse reaction	[(Rate w/o reverse reaction) – (Rate with reverse reaction)/Rate w/o reverse reaction]%	
	HTC1	HTC2
Dry-feed coal-derived syngas	19	11
Slurry-feed coal-derived syngas	58	34
Backend of membrane reactor	73	46
Backend of WGS reactor	88	76

3.4. Significance of reverse WGS reaction over HTC1 and HTC2

The above rate expressions imply that the presence of CO_2, and to a lesser extent H_2, in the syngas can have a significant effect on the CO conversion rate, particularly for high concentrations of CO_2 and H_2. This is due to the rate of the reverse WGS reaction increasing significantly as the concentrations of CO_2 and H_2 increase. Table 7 shows the effect of the reverse WGS reaction on the overall rate of the WGS reaction over HTC1 and HTC2. It shows the difference in the overall rates with and without the reverse WGS reaction expressed as a percentage of the rate without the reverse reaction.

Thus with the syngas from a dry-feed gasifier (with a composition as shown in Table 2) the reverse reaction has relatively less effect on CO conversion rate at the front-end of the WGS reactor especially with HTC2 (only 11%). However, with the syngas from a slurry-feed gasifier (Table 2) the reaction rate is reduced by 58% using HTC1 and 34% using HTC2 due to the higher contribution of the reverse reaction resulting from the higher concentrations of CO_2 and H_2.

At the backend of a conventional WGS reactor, using HTC1 and HTC2, the CO conversion rate is about 88% and 76% lower respectively as a result of the reverse reaction. However in a membrane reactor the removal of the H_2 reduces the impact of the reverse WGS reaction so that the reduction in CO conversion rate is relatively small especially over HTC2 (only about 46%) due to less-negative reaction order with respect to CO_2. Thus in addition to driving the equilibrium to the right, removal of H_2 in a membrane reactor can have a beneficial effect on the kinetics of the WGS reaction. This may reduce the size of reactor required provided that the heat release from the WGS reaction can be managed.

While increasing CO_2 concentration will have a negative effect on the CO conversion rate, the fact that the order of the reaction with respect to CO_2 is constant over the entire range of conditions investigated (see Fig. 3) indicates that there is no additional inhibition effect from high CO_2 concentrations other than that resulting from the reverse WGS reaction. This again implies that the use of a membrane reactor with in situ H_2 separation is potentially a viable alternative for conducting the WGS reaction without the need for a separate downstream H_2 recovery step.

4. Conclusions

As the compositions of two commercial catalysts used in this study are similar, it is not surprising that comparable performance

of HTC1 and HTC2 with the four selected gas inlet compositions is observed. For both HTC1 and HTC2 the highest WGS reaction rate was achieved under conditions where the CO concentration was at its maximum, i.e., with the composition simulating a syngas from a dry-feed coal-fired gasifier. The rate of CO conversion decreased as the CO concentration decreased and the concentrations of CO_2 and H_2 increased, conditions relevant to the backend of a WGS reactor.

The kinetics of the high-temperature WGS reaction over HTC1 and HTC2 are described well by a power-law rate equation with six parameters (i.e., pre-exponential factor, activation energy, and reaction orders with respect to both products and reactants). It was found that the role of the reverse WGS reaction is more significant with HTC1 than HTC2 at high CO_2 and H_2 concentrations, reflected in the more negative CO_2 and H_2 exponents for HTC1. The kinetic data showed that increasing H_2O concentration had a positive effect on the WGS reaction rate over HTC2 at H_2O: carbon ratios greater than 1.5.

As no additional inhibition effect from high CO_2 concentrations other than that resulting from the reverse WGS reaction was observed, the use of a membrane reactor with in situ H_2 separation is potentially a viable alternative for conducting the WGS reaction without the need for a separate downstream H_2 separation step.

Future work in this area will investigate in more detail possible reasons for the observed differences between these two samples. The next steps of this research will be to determine the performance of HTC1 and HTC2 at elevated pressures and to investigate the effects of impurities likely to be present in coal-derived syngases (e.g., H_2S, NH_3, Hg, etc.) on activities of HTC1 and HTC2. Such information has the potential to be useful in the design and development of high-temperature catalysts optimised for use in WGS reaction systems using coal-derived syngases.

Acknowledgements

The authors wish to acknowledge the support provided through the Centre for Low Emission Technology for this work. They would also like to acknowledge the assistance provided by Peter Beavis and Michael Mclnnes for construction of the rigs used in this work.

References

[1] C. Rhodes, G.J. Hutchings, A.M. Ward, Catal. Today 23 (1995) 43.
[2] P. Fott, J. Vosolsobe, V. Glaser, Coll. Czech. Chem. Commun. 44 (1979) 652.
[3] S.T. Oyama, G.A. Somorjai, J. Chem. Educ. 65 (1988) 765.
[4] M.V. Twigg, Catalyst Handbook, Wolfe Scientific, London, 1989.
[5] R.L. Keiski, T. Salmi, P. Niemesto, J. Ainassaari, V.J. Pohjola, Appl. Catal. A: Gen. 137 (1996) 349.
[6] J.M. Thomas, W.J. Thomas, Principles and Practice of Heterogeneous Catalysis, VCH, Weinheim, 1997.
[7] S. Oki, R. Mezaki, J. Phys. Chem. 77 (1973) 447.
[8] N. Amadeo, M. Laborde, Int. J. Hydrogen Energy 20 (1995) 949.
[9] E. Fiolitakis, H. Hofmann, J. Catal. 80 (1983) 328.
[10] C. Callaghan, I. Fishtik, R. Datta, M. Carpenter, M. Chmielewski, A. Lugo, Surf. Sci. 541 (2003) 21.
[11] D.S. Newsome, Catal. Rev. Sci. Eng. 21 (1980) 275.
[12] W.F. Podolski, Y.G. Kim, Ind. Eng. Chem. Proc. Des. Dev. 13 (1974) 415.
[13] Y. Choi, H.G. Stenger, J. Power Sources 124 (2003) 432.
[14] Y. Lei, N.W. Cant, D.L. Trimm, Chem. Eng. J. 114 (2005) 81.
[15] NETL, Texaco gasifier IGCC base cases, PED-IGCC-98-001, 2000.
[16] NETL, Shell gasifier IGCC base cases, PED-IGCC-98-002, 2000.
[17] Y. Lei, Ph.D. thesis, UNSW, 2005.
[18] C. Rhodes, G.J. Hutchings, Phys. Chem. Chem. Phys. 5 (2003) 2719.